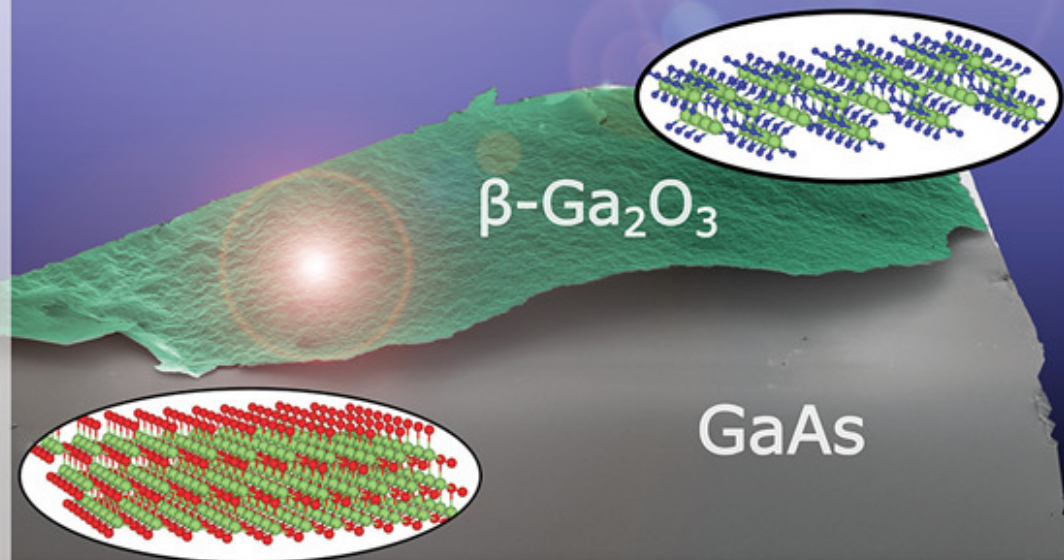
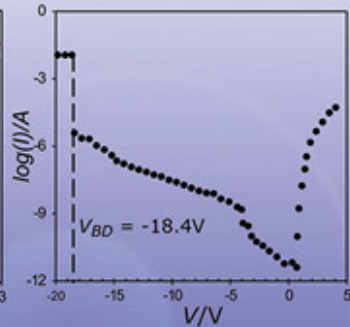
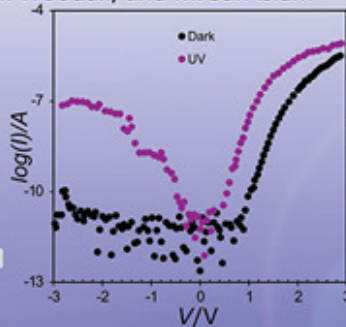
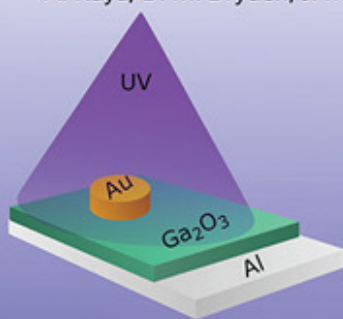


Spontaneous delamination via compressive buckling facilitates large-scale β - Ga_2O_3 thin film transfer from reusable GaAs substrates

A. Kaya, D. M. Dryden, J. M. Woodall, and M. Saif Islam



Spontaneous delamination via compressive buckling facilitates large-scale β -Ga₂O₃ thin film transfer from reusable GaAs substrates

Ahmet Kaya¹, Daniel M. Dryden², Jerry M. Woodall¹, and M. Saif Islam^{*1}

¹ Department of Electrical and Computer Engineering, University of California, Davis, CA, USA

² Department of Materials Science and Engineering, University of California, Davis, CA, USA

Received 22 February 2017, revised 11 May 2017, accepted 24 May 2017

Published online 20 June 2017

Keywords 2D film, nanoscale synthesis, optoelectronic devices, transfer printing, wide bandgap semiconductors

* Corresponding author: e-mail sislam@ucdavis.edu, Phone: +530-754-6732, Fax: +530-752-8428

The fabrication and transfer via spontaneous delamination of large-area, high-quality β -Ga₂O₃ nanoscale thin films with centimeter-scale dimensions is demonstrated via thermal oxidation of reusable GaAs substrates. The films are characterized by using X-ray diffraction, energy dispersive spectroscopy, Raman spectroscopy, and scanning electron microscopy. The film demonstrates good mechanical flexibility facilitating reliable transfer. The β -Ga₂O₃ film's optical band gap and Schottky barrier height with gold are 4.8 and

1.03 eV, respectively. Electrical and optical properties of the transferable β -Ga₂O₃ thin films exhibit a potential for application in solar-blind photodetectors. The scale of the β -Ga₂O₃ films transferred herein exceeds what the research community has reported to-date by more than four orders of magnitude. The macroscopic dimensions of the transferred films may offer a remedy for the low thermal conductance of β -Ga₂O₃ via transfer onto substrates with high thermal conductivity.

© 2017 WILEY-VCH Verlag GmbH & Co. KGaA, Weinheim

1 Introduction Wide-bandgap semiconductors including GaN and SiC have made tremendous progress in replacing silicon-based electronics in applications that call for low reverse leakage current, high breakdown voltage, or UV light selectivity. Beta-gallium oxide (β -Ga₂O₃), despite its relative technological immaturity, has demonstrated the potential to exceed the performance of GaN or SiC devices, thanks to its high breakdown field [1] and large figure of merit for high-frequency applications [2] both arising from its wide band gap of 4.8 eV [3]. Transistors with high breakdown voltage [2, 4–7] and high temperature handling capability have been demonstrated at the single-device scale. Applications of such transistors include conversion, distribution and management of electrical power in the grid and in heavy-duty electric motor drives for automotive engines and industrial plants. There has additionally been substantial recent interest in β -Ga₂O₃ for solar-blind UV detectors [8–11], gas sensors, [12] photocatalysts, [13, 14] substrates for the epitaxial growth of GaN and related III-nitride LEDs [15], and other applications.

The primary shortcoming of β -Ga₂O₃ is its low thermal conductivity, approximately an order of magnitude lower than that of GaN or SiC [5, 7, 16]. This can be overcome by limiting the β -Ga₂O₃ film thickness to the nanoscale, and β -Ga₂O₃ film growth on or transfer to a thermally conductive substrate such as silicon carbide (Table 1).

Several growth methods for β -Ga₂O₃ have been demonstrated, including molecular beam epitaxy (MBE) [16, 17], laser molecular beam epitaxy (LMBE) [18], pulsed laser deposition (PLD) [19], magnetron sputter deposition [20], laser ablation electron beam evaporation [21], plasma enhanced atomic layer deposition (PEALD) [22], vapor phase epitaxy [23], ultrasonic spray [24], MOCVD [25], float zone (FZ) [4], and sol-gel processing [26]. The straightforward growth of β -Ga₂O₃ on a substrate is hampered by its relative structural complexity versus the wurzitic, zincblende, or A4 structures typical of commonly used III–V and group IV semiconductors. In contrast β -Ga₂O₃ is monoclinic, belonging to the low-symmetry space group C2/m, making single-crystal

Table 1 Thermal conductivities of semiconductor materials and common substrates.

material	thermal conductivity /W · m ⁻¹ · K ⁻¹
β-Ga ₂ O ₃	13 [5]
GaAs	55 [4]
GaN	150–200 [5]
SiC	360–400 [5]
Si	150 [5]
Al ₂ O ₃	36 [45]
304 stainless steel	15 [46]
diamond	1000 [4]

and large-area growth difficult on many commonly used substrates. While β-Ga₂O₃ single-crystal substrates are available, they are cost-prohibitive for many applications and have poor thermal conductivity. The ability to grow and delaminate large scale β-Ga₂O₃ films from their growth substrate would allow for the transfer of the film onto an inexpensive and thermally conductive substrate of choice for device formation, and the reuse of the growth template. Thus, in a growing market for β-Ga₂O₃ electronics [1] with a lack of affordable, high quality, large, native substrates, critical to the implementation of such devices is the ability to grow and transfer large-area crystalline β-Ga₂O₃ films.

Graphene is the model material in which large-area thin films may be achieved by mechanical exfoliation from the bulk [27, 28]. Here, however, the peel-off of graphene layers from bulk graphite is eased by weak inter-plane van der Waals bonding [29, 30], whereas β-Ga₂O₃ is strongly bonded in all three dimensions. Nonetheless, moderate success in the exfoliation of β-Ga₂O₃ sheets from the bulk has been achieved [5, 31, 32], with Mitdank et al. [31] demonstrating the fabrication of thin β-Ga₂O₃ flakes 4 μm wide and 14 μm long exfoliated from bulk crystals grown using the Czochralski method. Even so, this method is not transferable to larger areas, and can only be used for fabricating one or a few devices at one time. For any fabrication technique to be feasible at the commercial scale,

it must be low-cost, scalable to areas of millimeter dimensions or greater, and produce films of sufficient material quality for the fabrication of electronic devices.

Film stress is a major source of defects and failure in thin film technology. One source of stress commonly present in films grown at elevated temperatures is that induced by differential thermal expansion, given by Eq. (1):

$$\sigma_T = \frac{E}{1 - \nu} \Delta\bar{\alpha}\Delta T \quad (1)$$

where σ_T is the thermally induced stress, E is the Young's modulus of the film, ν is the Poisson's ratio, $\Delta\bar{\alpha}$ is the average differential coefficient of thermal expansion between the film and substrate material over the relevant temperature range, and ΔT is the change in temperature. Over large temperature ranges or large differences in thermal expansion coefficients, extremely large stresses may be imposed on the film, resulting in the case of compressive stresses in buckling, cracking, or delamination. It is generally sought to avoid these stresses and effects whenever high film-substrate adhesion is desired. These forces may nonetheless be exploited in cases where delamination is desired to achieve film liftoff or the fabrication of complex 3-dimensional structures [33, 34]. In the case of β-Ga₂O₃ on GaAs, the coefficients of thermal expansion differ by a factor between 2 and 4.3 [35, 36], allowing considerable compressive stresses to come to bear on the β-Ga₂O₃ film even when the system is cooled over a relatively limited temperature range. Careful control over the growth temperature, duration, and cooling rate may therefore be used to control the stresses present in the system and the subsequent ease of oxide film delamination upon cooling.

In this study, we demonstrate a new method of growing very large-area β-Ga₂O₃ films via thermal oxidation of (111) n-GaAs. We have successfully grown films with more than four orders of magnitude larger size than those previously reported in the research community, transferred

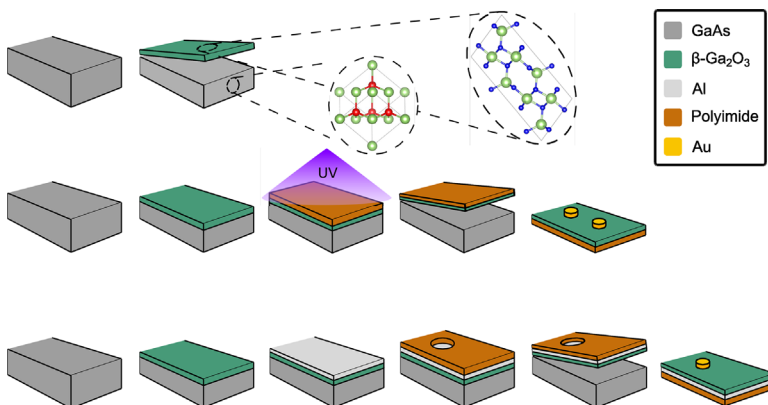


Figure 1 Process flow for the fabrication of β-Ga₂O₃ films and devices via three methods. Top: GaAs is oxidized in a furnace at 830 °C to form a film of β-Ga₂O₃, and the film spontaneously delaminates upon cooling. Middle: GaAs is oxidized in a furnace at 730 °C to form a film of β-Ga₂O₃, and a polyimide film is deposited and cured under UV light. The film is used to mechanically delaminate the β-Ga₂O₃ from the surface, and Au contacts are deposited to form a MSM device. Bottom: GaAs is oxidized in a furnace at 730 °C to form a film of β-Ga₂O₃, and a film of Al is deposited to form an ohmic contact. The film stack is delaminated using polyimide tape with a hole to facilitate electrical connection to the Al contact, and an Au contact is deposited on the back side of the β-Ga₂O₃ to form a Schottky diode.

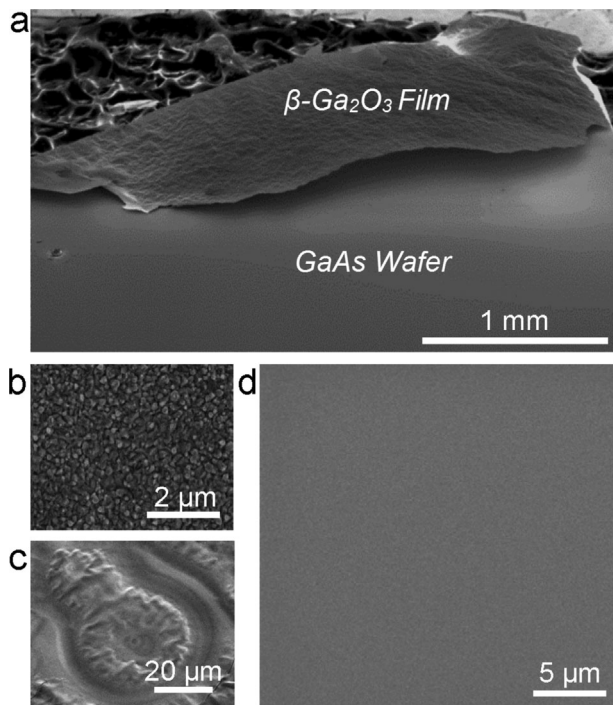


Figure 2 a) β - Ga_2O_3 film on GaAs grown at 830°C and spontaneously delaminated. b) Backside of film grown at 830°C , showing well-defined grain structure. c) The top surface of β - $\text{Ga}_2\text{O}_3/\text{GaAs}$ grown at 730°C without Ar carrier gas, showing circular structures resulting from Ga puddle formation and subsequent oxidation. d) The surface of β - Ga_2O_3 grown on GaAs at 730°C , and mechanically delaminated via the deposition and curing of a polyimide film. Films grown under these conditions are nanocrystalline and relatively defect-free.

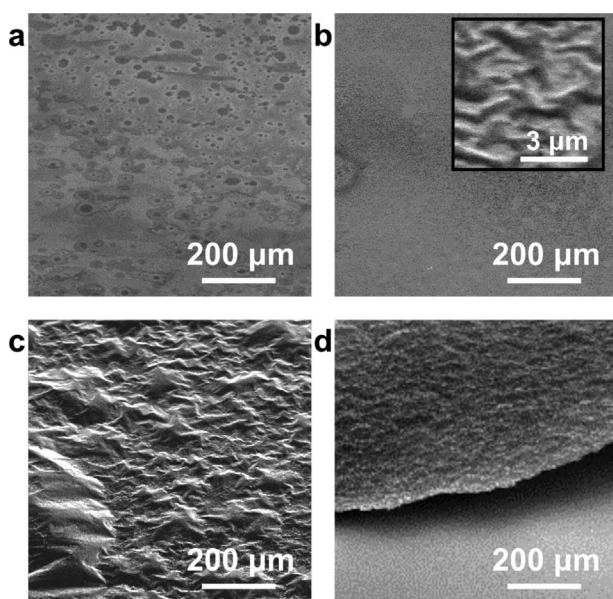


Figure 3 a) SEM micrograph of film surfaces grown at a) 670°C , b) 700°C (inset: closeup of surface texture), c) 800°C and d) 830°C .

these films via spontaneous or mechanical delamination, and characterized them structurally, spectroscopically, electrically, and optically. This new method of thermal stress-assisted delamination allows for the low-cost fabrication and transfer of centimeter-scale β - Ga_2O_3 films to arbitrary substrates, preferably onto substrates with high thermal conductance.

2 Experimental

2.1 Oxide film growth N-type GaAs substrates with (111) orientation were placed in a horizontal quartz tube furnace, which was continuously pumped down to 640 torr. Argon gas was used at a flow rate of 100 sccm, while the residual O_2 in the system acted as the reaction gas. Films were grown at temperatures between 685 – 830°C . The furnace temperature was ramped up from room temperature over a 150-min period, held at the growth temperature for 50 min, and then ramped down to room temperature over a 150-min period.

2.2 Oxide film delamination Films grown at 830°C were observed to naturally delaminate from the surface (Fig. 1, top) while films grown at 700 or 730°C were mechanically delaminated via the drop-casting and curing of a polyimide film (Fig. 1, middle) or removal using polyimide tape. Polyimide resin (Fujifilm, Japan) was drop casted onto the as-grown β - Ga_2O_3 layer, then the sample was spincoated on a Laurell WS-650 spin processor (Laurell Technologies Corporation, USA) for 25 s at 3000 rpm. The polyimide layer was then cured under UV illumination from a Dymax Bluewave75 UV curing lamp (Dymax Corporation, USA). The films were then mechanically delaminated from the GaAs substrates.

2.3 Characterization Films and film stacks were characterized in their free-standing form without being transferred to a wafer substrate. Scanning electron microscopy (SEM) and EDS were performed with a Philips/FEI XL30 microscope (FEI, USA) and EDAX detector (EDAX Inc., USA) and analyzed using EDAX Genesis software. XRD was performed with a Bruker D8 Discover diffractometer (Bruker, USA) on β - Ga_2O_3 films grown at 800°C on GaAs prior to delamination in order to maintain film-substrate orientation information. Raman spectra were collected using an Andor spectrometer (Andor Technology Ltd, UK). Optical characterizations were performed using an Ocean Optics USB 2000+ spectrometer (Ocean Optics, USA) in transmission geometry; these measurements were performed on the spontaneously delaminated film sample grown at 830°C so as to measure only the absorbance of the β - Ga_2O_3 film rather than the polyimide or aluminum. For electrical characterizations, Au contacts with 1 mm diameter and a thickness of 150 nm and Al films with a thickness of 100 nm were deposited in a CHA Autotech II electron beam evaporator (CHA Industries, Inc., USA) on the films grown at 730°C . Electrical and optoelectronic characterizations were performed using an

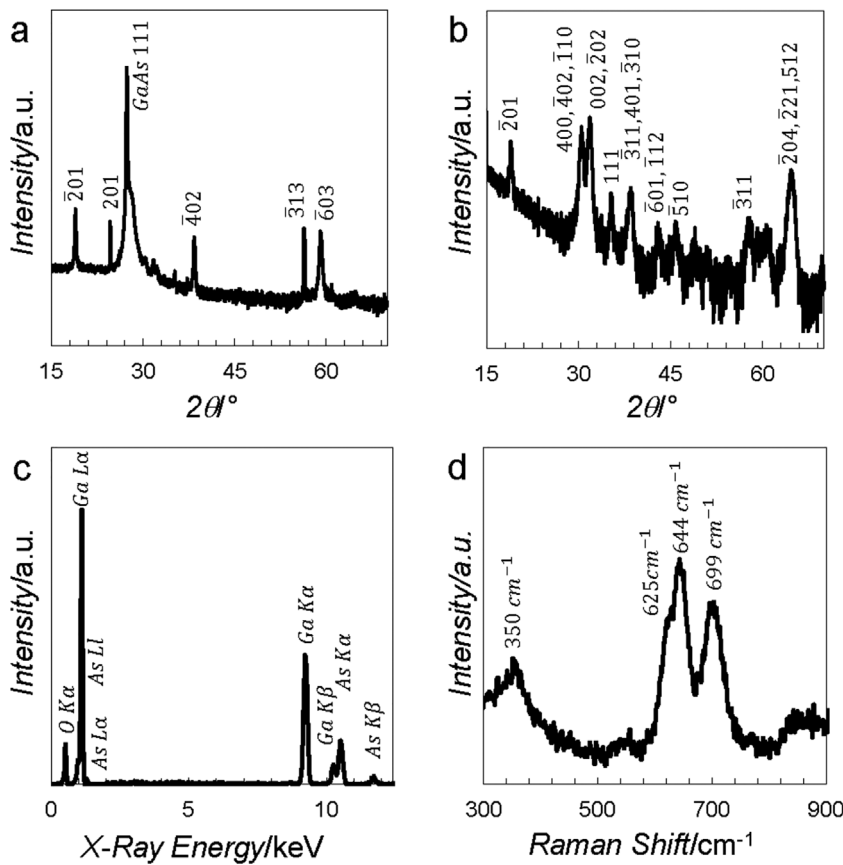


Figure 4 a) θ - 2θ x-ray diffraction (XRD) pattern, indexed in comparison to PDF 00-041-1103, for β - Ga_2O_3 grown at 800°C on a (111) GaAs substrate. b) glancing angle 0.6° XRD pattern for β - Ga_2O_3 grown at 800°C on a (111) GaAs substrate, indexed in comparison to PDF 00-041-1103. c) energy dispersive spectroscopy (EDS) measurement of for β - Ga_2O_3 grown at 800°C on GaAs indicating the presence of Ga, O, and As in the sample, and d) Raman spectrum for β - Ga_2O_3 grown at 800°C .

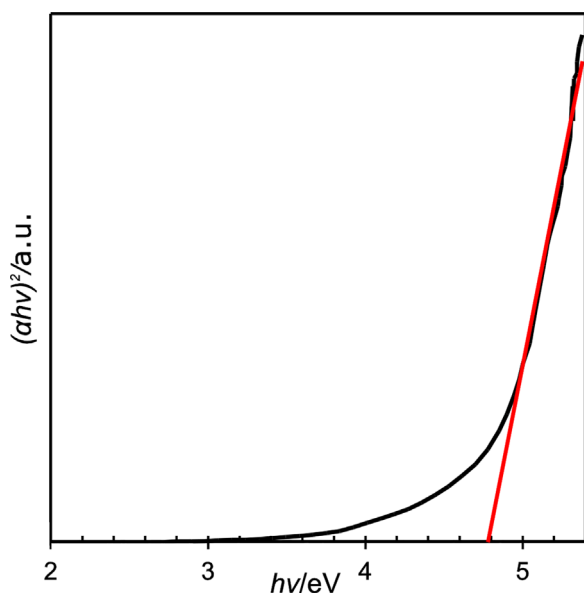


Figure 5 a) Optical absorbance of the free-standing β - Ga_2O_3 film grown at 830°C , plotted as $(\alpha h\nu)^2$ versus photon energy $h\nu$. The red line is a linear extrapolation of the linear portion of the absorbance plot, indicating a direct band gap energy of 4.8 eV .

HP4155B Semiconductor Parameter Analyzer (Hewlett-Packard, USA) at ambient temperature in dark conditions and under UV illumination from a Dymax Bluewave75 UV lamp.

3 Results and discussion

3.1 Delamination and physical characterization The β - Ga_2O_3 films achieved via thermal oxidation and transfer (Fig. 1) had dimensions in the centimeter scale per side, which is substantially larger than demonstrated in previous reports [5, 31]. The surface quality, thickness, and grain structure of the β - Ga_2O_3 film as observed by scanning electron microscopy (SEM) was found to change with growth temperature (Fig. 2). Films grown at 830°C (Fig. 2a and b) had a thickness of about 70 nm , as estimated from cross-sectional SEM images of the partially delaminated films, and polycrystalline texture with well-defined grains as small as 50 nm (Fig. 2b). Circular formations (Fig. 2c) can be seen in some films grown without Ar gas and lend insight into the film formation process. These formations likely result from the formation of Ga droplets via thermal decomposition of the GaAs, [37–39] that are subsequently oxidized into β - Ga_2O_3 concurrent with the evaporation of As [21]. Films grown

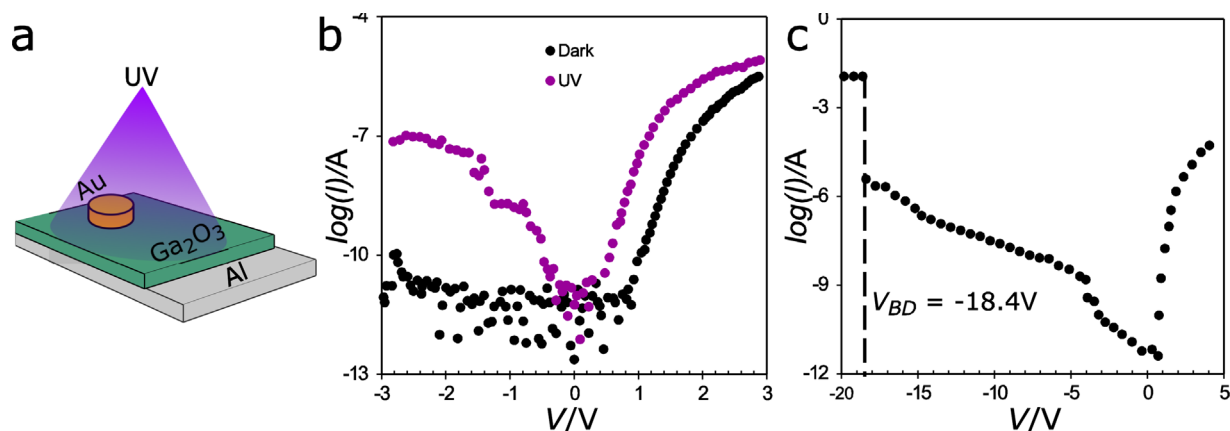


Figure 6 a) Schematic of Schottky diode (SD) structure, b) I–V behavior without (black) and with (purple) Xenon arc lamp UV illumination of Au/ β -Ga₂O₃/Al SDs fabricated from β -Ga₂O₃ grown at 730 °C, showing a substantial photoresponse, and c) dark I–V curve of a SD fabricated from β -Ga₂O₃ grown at 730 °C, showing a reverse breakdown voltage of 18.4 V.

at lower temperatures 730 °C (Fig. 2d) had a fine, nanocrystalline grain structure and reduced thickness proportional to growth temperature. Both film thickness and the effects of thermal differential stress increased with growth temperature (Fig. 3). β -Ga₂O₃ Films grown at 670 °C (Fig. 3a) did not fully coalesce into a single continuous film. At 700 °C (Fig. 3b) the film completely covered the GaAs substrate but did not spontaneously delaminate; however, stress buckling (Fig. 3b, inset) was visible at the microscale. At 800 °C (Fig. 3c), the film partially delaminated due to stress, demonstrating both micro- and macro-scale buckling. Films grown at 830 °C (Fig. 3d) spontaneously delaminated from the GaAs surface. Some films fractured as well during delamination; after delamination and cooling all films were found to be mechanically stable. Films grown at lower temperatures 700 °C and 730 °C buckled at the microscale but did not fully delaminate. Such films were easily mechanically delaminated via the drop-casting and curing of a polyimide film on the surface to aid with peel-off (see Experimental section). During cooling, the oxide film experiences extremely high compressive strains due to the large

disparity in coefficient of thermal expansion between GaAs and β -Ga₂O₃ (an α_L between 1.5×10^{-6} and 3.5×10^{-6} K⁻¹ for β -Ga₂O₃ [35] and an α_L of 6.5×10^{-6} K⁻¹ for GaAs) [36], which results in a similarly large stress due to the high Young's modulus of 230 GPa for β -Ga₂O₃ [40]. This stress provides the energy necessary to delaminate the film. In the case of high-temperature growth, and therefore a large ΔT , these stresses are high enough to fully delaminate the film, and in some cases fracture it as well. Growth at lower temperatures reduces the differential stresses while still maintaining large-area films in good mechanical condition.

3.2 Structural and material characterization

Multiple material characterization techniques (Fig. 4) positively identify the sample film grown at 800 °C as polycrystalline β -Ga₂O₃. XRD performed in the standard θ - 2θ geometry shows strong texturing in the $\bar{2}01$ direction (Fig. 4a), while glancing-angle XRD, which maximizes film signal at the cost of orientation information, produced results (Fig. 4b) which are clearly consistent with polycrystalline β -Ga₂O₃, as referenced against the

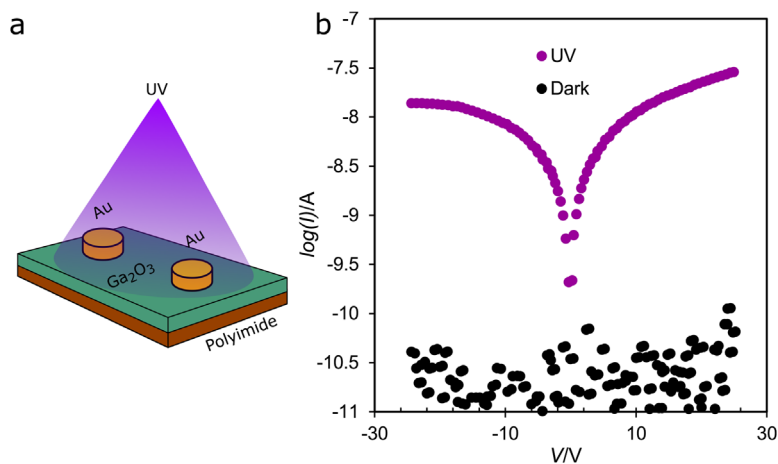


Figure 7 a) Schematic of Au/ β -Ga₂O₃/Au metal-semiconductor metal (MSM) structure on polyimide backing. b) I–V behavior without (black) and with (purple) Xenon arc lamp UV illumination of Au/ β -Ga₂O₃/Au MSM fabricated from β -Ga₂O₃ grown at 730 °C, showing a substantial photoresponse.

Table 2 Electrical parameters of an Au/ β -Ga₂O₃/Al Schottky diode fabricated from β -Ga₂O₃ grown at 730 °C, as determined from I - V curves and the Norde method [42, 43].

Φ_B (Norde)	Φ_B (I - V)	R_S (Norde)	n	V_{BC}
1.03 eV	1.04 eV	3 M Ω	2.7	18.4 V

International Center for Diffraction Data (ICDD) standard PDF

00-041-1103 [41]. The (111) GaAs//($\bar{2}$ 01) β -Ga₂O₃ epitaxial relationship is consistent with literature results; further work would be useful in elucidating the in-plane orientation relationship of the film when grown using this method. Energy dispersive spectroscopy (EDS) measurements (Fig. 4c) further confirm qualitatively the presence of Ga, O, and As in the sample. Raman spectroscopy (Fig. 4d) was also performed on the oxide film. Distinct features can be seen at 350, 625, 644, and 699 cm⁻¹. The first two are consistent with features seen in bulk β -Ga₂O₃ crystals [38] while the latter two are in good agreement with blue-shifted features reported by Rao et al. [39] in β -Ga₂O₃ nanowires. Differences in the overall stress state versus that reported by Rao et al. [39] would explain why certain peaks are blue-shifted while others are not. Further research is warranted to elucidate the specific origins and stress dependence of these Raman features.

3.3 Optical and electrical device characterization The β -Ga₂O₃ film on GaAs grown at 830 °C and spontaneously delaminated was characterized optically (Fig. 5), demonstrating visible-range transmission exceeding 80%, which is critical for applications in solar-blind UV detection. The direct band gap E_g was determined to be 4.8 eV by linear fitting of $(\alpha h\nu)^2$ versus $(h\nu)$, in good agreement with literature values [8, 19].

Au/ β -Ga₂O₃/Al Schottky diodes (SDs) (Fig. 6) and Au/ β -Ga₂O₃/Au metal-semiconductor-metal (MSM) photodetectors (Fig. 7) were fabricated to determine the electronic quality of the films. The film grown at 730 °C was used for device fabrication, as it provided the sufficient thickness and appropriate ease of handling. The current-voltage (I - V) characteristics were measured in dark conditions and under UV illumination for both the MSM and SD devices (Figs. 6b and 7b, respectively). The MSM diode under visible and near-visible monochromatic illumination showed results comparable to the dark current, wherein the β -Ga₂O₃ is almost an insulator, indicating good suitability for solar-blind applications. Photocurrents were strongly excited by UV light. The diode ideality factor n , barrier height ϕ_B , and breakdown voltage V_{BD} (Fig. 6c) for the Au/ β -Ga₂O₃/Al SDs were obtained by analyzing the I - V characteristics in dark conditions; additionally the ϕ_B and series resistance R_s values for the SDs with large R_s were obtained using the method developed by Norde [42] and modified by Lien et al. [43] (Table 2). The ϕ_B and R_s

results are very close to previously reported values for Au/ β -Ga₂O₃ SDs [44]. The diode rectification factor, as defined as the ratio of currents at +3.9 and -3.9 V, was found to be 10⁵.

4 Conclusions Large-scale, high quality β -Ga₂O₃ thin films with dimensions in the centimeter scale were grown via thermal oxidation on reusable GaAs and mechanically delaminated for transfer onto alternative substrates. The films were characterized using X-ray diffraction, energy dispersive spectroscopy, Raman spectroscopy, and scanning electron microscopy. The transmittance of the films exceeded 80% in the visible region and the optical band gap was calculated as 4.8 eV. The films were then used to fabricate Au/ β -Ga₂O₃/Au MSM photodetectors and Au/ β -Ga₂O₃/Al Schottky diodes, and the electrical parameters of the thin film devices were determined. A strong photocurrent under UV illumination combined with high visible-range transmittance of the transferable β -Ga₂O₃ thin films demonstrates these films' potential for solar-blind photodetectors. The barrier height and ideality factor were measured as 1.04 eV and 2.7, respectively, from the forward bias I - V plot. The barrier height and series resistance were found to be 1.03 eV and 3 M Ω , respectively, using the Norde method. The ability to transfer thin layers of β -Ga₂O₃ to a desirable substrate and re-use the GaAs substrate holds potential for a breakthrough in the drastic cost reduction of β -Ga₂O₃ enabled devices. The greater than four orders of magnitude larger size of these grown and delaminated β -Ga₂O₃ films versus those previously reported in the literature addresses the important scalability and cost-performance ratio of the intended devices and systems. This demonstration offers motivation for further research toward the seamless transfer of β -Ga₂O₃ films and subsequent material growth and processes for high-power transistors, LEDs and solar-blind UV detector fabrication.

Acknowledgements Partial support from ARO (W911NF-14-4-0341) is gratefully acknowledged by the authors. Author 1 and Author 2 contributed equally to this work. The authors would like to thank Michael Lee for his assistance in obtaining high quality XRD data.

References

- [1] R. Stevenson, Gallium Oxide: Power Electronics' Cool New Flavor. IEEE Spectr. 2016.
- [2] H. Zhou, M. Si, S. Alghamdi, G. Qiu, L. Yang, and P. D. Ye, IEEE Electron Device Lett. **38**, 103 (2017).
- [3] H. He, R. Orlando, M. A. Blanco, R. Pandey, E. Amzallag, I. Baraille, and M. Rérat, Phys. Rev. B **74** (2006).
- [4] M. Higashiwaki, K. Sasaki, A. Kuramata, T. Masui, and S. Yamakoshi, Appl. Phys. Lett. **100**, 13504 (2012).

- [5] W. S. Hwang, A. Verma, H. Peelaers, V. Protasenko, S. Rouvimov, H. (Grace) Xing, A. Seabaugh, W. Haensch, C. V. de Walle, Z. Galazka, M. Albrecht, R. Fornari, and D. Jena, *Appl. Phys. Lett.* **104**, 203111 (2014).
- [6] T. Onuma, S. Fujioka, T. Yamaguchi, Y. Itoh, M. Higashiwaki, K. Sasaki, T. Masui, and T. Honda, *J. Cryst. Growth* **401**, 330 (2014).
- [7] M. Higashiwaki, K. Sasaki, A. Kuramata, T. Masui, and S. Yamakoshi, *Phys. Status Solidi A* **211**, 21 (2014).
- [8] M. Orita, H. Hiramatsu, H. Ohta, M. Hirano, and H. Hosono, *Thin Solid Films* **411**, 134 (2002).
- [9] F. Alema, B. Hertog, O. Ledyev, D. Volovik, G. Thoma, R. Miller, A. Osinsky, P. Mukhopadhyay, S. Bakhshi, H. Ali, and W. V. Schoenfeld, *Phys. Status Solidi A* 1600688 (2017).
- [10] D. Guo, H. Liu, P. Li, Z. Wu, S. Wang, C. Cui, C. Li, and W. Tang, *ACS Appl. Mater. Interfaces* **9**, 1619 (2017).
- [11] D. Y. Guo, H. Z. Shi, Y. P. Qian, M. Lv, P. G. Li, Y. L. Su, Q. Liu, K. Chen, S. L. Wang, C. Cui, C. R. Li, and W. H. Tang, *Semicond. Sci. Technol.* **32**, 03LT01 (2017).
- [12] H.-J. Lin, H. Gao, and P.-X. Gao, *Appl. Phys. Lett.* **110**, 43101 (2017).
- [13] Y. Ma, X. Zhao, M. Niu, W. Li, X. Wang, C. Zhai, T. Wang, Y. Tang, and X. Dai, *RSC Adv.* **7**, 4124 (2017).
- [14] C.-T. Shao, W.-Z. Lang, X. Yan, and Y.-J. Guo, *RSC Adv.* **7**, 4710 (2017).
- [15] S. Ito, K. Takeda, K. Nagata, H. Aoshima, K. Takehara, M. Iwaya, T. Takeuchi, S. Kamiyama, I. Akasaki, and H. Amano, *Phys. Status Solidi C* **9**, 519 (2012).
- [16] E. G. Villora, K. Shimamura, Y. Yoshikawa, T. Ujiie, and K. Aoki, *Appl. Phys. Lett.* **92**, 202120 (2008).
- [17] T. Oshima, N. Arai, N. Suzuki, S. Ohira, and S. Fujita, *Thin Solid Films* **516**, 5768 (2008).
- [18] M. Ai, D. Guo, Y. Qu, W. Cui, Z. Wu, P. Li, L. Li, and W. Tang, *J. Alloys Compd.* **692**, 634 (2017).
- [19] M. Orita, H. Ohta, M. Hirano, and H. Hosono, *Appl. Phys. Lett.* **77**, 4166 (2000).
- [20] M. Fleischer, S. Kornely, T. Weh, J. Frank, and H. Meixner, *Sens. Actuators B Chem.* **69**, 205 (2000).
- [21] N. C. Oldham, C. J. Hill, C. M. Garland, and T. C. McGill, *J. Vac. Sci. Technol. Vac. Surf. Films* **20**, 809 (2002).
- [22] H. Altuntas, I. Donmez, C. Ozgit-Akgun, and N. Biyikli, *J. Alloys Compd.* **593**, 190 (2014).
- [23] V. Gottschalch, K. Mergenthaler, G. Wagner, J. Bauer, H. Paetzelt, C. Sturm, and U. Teschner, *Phys. Status Solidi A* **206**, 243 (2009).
- [24] A. Ortiz, J. C. Alonso, E. Andrade, and C. Urbiola, *J. Electrochem. Soc.* **148**, F26 (2001).
- [25] M. Hellwig, K. Xu, D. Barreca, A. Gasparotto, M. Winter, E. Tondello, R. A. Fischer, and A. Devi, *Eur. J. Inorg. Chem.* **2009**, 1110 (2009).
- [26] M. R. Mohammadi and D. J. Fray, *Acta Mater.* **55**, 4455 (2007).
- [27] X. Li, W. Cai, J. An, S. Kim, J. Nah, D. Yang, R. Piner, A. Velamakanni, I. Jung, E. Tutuc, S. K. Banerjee, L. Colombo, and R. S. Ruoff, *Science* **324**, 1312 (2009).
- [28] W. H. Lee, J. Park, S. H. Sim, S. B. Jo, K. S. Kim, B. H. Hong, and K. Cho, *Adv. Mater.* **23**, 1752 (2011).
- [29] P. L. de Andres, R. Ramirez, and J. A. Vergés, *Phys. Rev. B* **77** (2008).
- [30] W. Wang, S. Dai, X. Li, J. Yang, D. J. Srolovitz, and Q. Zheng, *Nat. Commun.* **6**, 7853 (2015).
- [31] R. Mitdank, S. Dusari, C. Bülow, M. Albrecht, Z. Galazka, and S. F. Fischer, *Phys. Status Solidi A* **211**, 543 (2014).
- [32] J. Kim, S. Oh, M. A. Mastro, and J. Kim, *Phys. Chem. Chem. Phys.* **18**, 15760 (2016).
- [33] S. Xu, Z. Yan, K.-I. Jang, W. Huang, H. Fu, J. Kim, Z. Wei, M. Flavin, J. McCracken, R. Wang, A. Badea, Y. Liu, D. Xiao, G. Zhou, J. Lee, H. U. Chung, H. Cheng, W. Ren, A. Banks, X. Li, U. Paik, R. G. Nuzzo, Y. Huang, Y. Zhang, and J. A. Rogers, *Science* **347**, 154 (2015).
- [34] K. Nan, H. Luan, Z. Yan, X. Ning, Y. Wang, A. Wang, J. Wang, M. Han, M. Chang, K. Li, Y. Zhang, W. Huang, Y. Xue, Y. Huang, Y. Zhang, and J. A. Rogers, *Adv. Funct. Mater.* **27**, 1604281 (2017).
- [35] F. Orlandi, F. Mezzadri, G. Calestani, F. Boschi, and R. Fornari, *Appl. Phys. Express* **8**, 111101 (2015).
- [36] J. Bąk-Misiuk, H. G. Brühl, W. Paszkowicz, and U. Pietsch, *Phys. Status Solidi A* **106**, 451 (1988).
- [37] T. D. Lowes and M. Zinke-Allmang, *J. Appl. Phys.* **73**, 4937 (1993).
- [38] K. Shorlin and M. Zinke-Allmang, *Surf. Sci.* **601**, 2438 (2007).
- [39] S. A. Chambers, *Surf. Sci. Rep.* **39**, 105 (2000).
- [40] TAMURA Corporation, Single-Crystal Gallium Oxide Substrates.
- [41] Y. Zhao and R. L. Frost, *J. Raman Spectrosc.* **39**, 1494 (2008).
- [42] H. Norde, *J. Appl. Phys.* **50**, 5052 (1979).
- [43] C.-D. Lien, F. C. T. So, and M.-A. Nicolet, *IEEE Trans. Electron Devices* **31**, 1502 (1984).
- [44] M. Mohamed, K. Irmscher, C. Janowitz, Z. Galazka, R. Manzke, and R. Fornari, *Appl. Phys. Lett.* **101**, 132106 (2012).
- [45] J. F. Shackelford and R. H. Doremus, *Ceramic and Glass Materials: Structure, Properties, and Processing* (Springer, Boston, 2008) p. 14.
- [46] J. N. Sweet, E. P. Roth, and M. Moss, *Int. J. Thermophys.* **8**, 593 (1987).